

Circularly Polarized Luminescence and Circular Dichroism from Si–Si-Bonded Network Polymers

Satoshi Fukao and Michiya Fujiki*

Graduate School of Materials Science, Nara Institute of Science and Technology, 8916-5 Takayama, Ikoma, Nara 630-0036, Japan

Received July 2, 2009; Revised Manuscript Received September 2, 2009

ABSTRACT: We demonstrated the first circularly polarized luminescence (CPL) and circular dichroism (CD) spectra of three new Si–Si-bonded network polymers bearing the chiral alkyl side groups poly[(*S*)-2-methylbutylsilyl] (**1S**), poly[(*R*)-3,7-dimethyloctylsilyl] (**2R**), poly[(*S*)-3,7-dimethyloctylsilyl] (**2S**), and, for comparison, poly(*n*-pentylsilyl), which bears an achiral alkyl side group (**3**). These polymers were successfully prepared by Na-mediated condensation of the corresponding alkyltrichlorosilanes with the help of crown ether. It was revealed that only **1S**, which bears a β -branched chiral group, clearly showed an intense CPL signal at ~ 570 nm with a quantum yield of $\sim 1\%$, along with its corresponding Cotton CD signals in tetrahydrofuran at room temperature. In contrast, **2R** and **2S**, which possess γ -branched chiral groups, did not show any CPL signal, though they did show the CD bands. As expected, **3** did not show CPL or CD signals. The β -branched chiral side chain was needed to provide the intense CPL band in the visible region and to effectively induce chirally distorted Si–Si-bonded structures in Si–Si-bonded network polymers.

Introduction

The generation, amplification, and switching of circularly polarized luminescence (CPL) and circular dichroism (CD) from polymers,¹ small molecules,² and solid crystals³ have received considerable theoretical and experimental attention. CPL is inherent to asymmetric fluorophores in the excited state, whereas CD is due to asymmetric chromophores in the ground state.⁴

In recent years, it has been established that the dimensionality of semiconductors is directly related to pronounced photophysical properties. A typical example is a family of Si–Si-bonded materials.⁵ Crystalline silicon (*c*-Si), an achiral three-dimensional structure, is a poor emitter with a quantum yield (Φ) of 0.01% at 300 K, with no reports of CPL or CD signals. However, since the early reports of fairly efficient photoluminescence (PL) in the visible–near-infrared (vis–NIR) region of nanocrystalline Si (*nc*-Si)⁶ and porous Si,⁷ several low-dimensional Si–Si-bonded systems have proven to be fascinating materials for tuning and controlling PL properties throughout the UV–vis–NIR region, both theoretically⁵ and experimentally.^{6–13} These materials have included zero-dimensional *nc*-Si,⁸ one-dimensional (1D) polysilane,⁹ two-dimensional (2D) Si–Si-bonded networks such as organopolysilyl (SNP),¹⁰ siloxene,¹¹ and Si/SiO₂ superlattices,¹² and branched linear polysilanes.¹³ With the exception of 1D helical polysilanes bearing chiral groups,^{9c–e} these low-dimensional structures are typically achiral, leading to no optical activity, including CD and CPL signals.

Although SNP is a soluble model polymer of amorphous Si (*a*-Si) and 2D-Si nanosheets,^{5,10} further studies of the synthesis and (chir)optical properties of SNP with chiral side groups have not yet been carried out. This is because ideal 2D- and *a*-Si-like structures have long been thought to be achiral. The only exception to this rule is ladder-like oligosilanes, consisting of fused four-member Si–Si-bonded rings with achiral isopropyl groups, which adopt a helical conformation in the solid state and a presumably CD-silent helical conformation in THF solution.¹⁴

Here we report the first chiroptical (CPL and CD) spectra of three new SNPs bearing the chiral alkyl side groups poly[(*S*)-2-methylbutylsilyl] (**1S**), poly[(*R*)-3,7-dimethyloctylsilyl] (**2R**), poly[(*S*)-3,7-dimethyloctylsilyl] (**2S**), and, for comparison, the achiral group poly(*n*-pentylsilyl) (**3**) (Chart 1). It was revealed that only **1S** bearing β -branched chiral groups clearly showed an intense CPL signal at ~ 570 nm with Φ of $\sim 1\%$, along with its corresponding Cotton CD signals in tetrahydrofuran (THF) at room temperature. In contrast, **2R** and **2S**, which possess γ -branched chiral groups, did not show any CPL signals, though they did show the CD bands. As expected, **3** did not show CPL or CD signals.

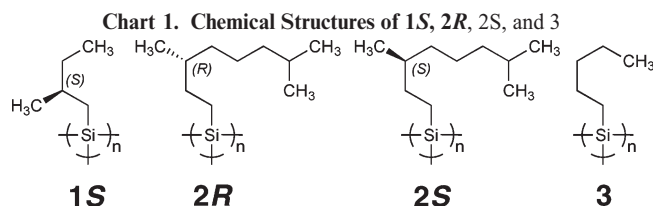
Results and Discussion

Scheme 1 shows the general synthetic scheme for the SNPs studied in this work. Note that the use of Na metal with catalytic 12-crown-4 removed the need for ultrasonic wave (USW) irradiation in the preparation of these SNPs, thus providing milder and safer conditions.^{10f,e} In comparison, a liquid NaK alloy and USW irradiation were originally applied in the preparation of the first SNP.^{10a,b} Table 1 gives brief synthetic data for the four SNPs. Although the values of M_w and PDI for **1S**, **2R**, and **2S** are similar, **3** (with a nonbranched side chain) had a larger M_w and a broader PDI. This trend has already been observed in previous works¹⁰ and may be related to the degree of steric interaction between the side chains.

Figure 1 shows the subtracted ²⁹Si NMR spectra of **1S**, **2R**, **2S**, and **3** in CDCl₃ along with CDCl₃ alone at room temperature. Three broad ²⁹Si resonances of the blank sample around -100 , -80 , and -50 ppm were attributed to ²⁹Si-containing glass in the NMR tube and probe. By subtracting the ²⁹Si NMR spectrum of the blank sample from the NMR spectra for **1S**, **2R**, **2S**, and **3**, ²⁹Si NMR spectra for these SNPs were obtained.

A broad ²⁹Si resonance near -55 ppm was commonly seen for these SNPs. Although this ²⁹Si resonance may overlap with the ²⁹Si resonance at -50 ppm, the remaining two ²⁹Si resonances at -100 and -80 ppm almost disappeared. The ²⁹Si resonance of the four SNPs near -55 ppm appears to be characteristic of

*Corresponding author: Fax 81-743-72-6049; Tel 81-743-72-6040; e-mail fujikim@ms.naist.jp.



Scheme 1. Polymerization Scheme for the SNPs

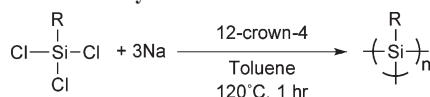


Table 1. Synthetic Data for the Network Polysilynes

polymer	$M_w \times 10^{-3}$	PDI	yields (%)	color and state
1S	4.3	1.5	24.1	yellow solid
2R	4.0	1.4	26.7	yellow paste
2S	4.8	1.8	29.4	yellow paste
3	32.0	4.4	22.0	orange-yellow solid

^a M_w and M_n values were estimated via calibration of chain-like polystyrene standards. However, actual molecular weights may be higher due to underestimation of the hydrodynamic radii of the network structures compared to polystyrene standards with chain-like structure.

several SNPs bearing *n*-alkyl groups reported previously.^{10b,f,15} The broadness of the peak is due to a solid-like structure with a very restricted skeletal motion.^{10b,f}

Indeed, Furukawa et al.^{10f} and Bianconi et al.^{10b} showed very broad solution ²⁹Si NMR signals with line widths of ca. 20–30 ppm from *n*-hexylpolysilyne and *n*-propylpolysilyne. The former was prepared by Na-mediated condensation of *n*-hexyltrichlorosilane and the latter by Na–K-mediated condensation of *n*-propyltrichlorosilane. Bianconi et al.^{10b} further compared these results with the corresponding solid-state CP/MAS ²⁹Si NMR signals of *n*-propylpolysilyne, *n*-butylpolysilyne, and *n*-hexylpolysilyne. When in the solid state, these SNPs have broad ²⁹Si NMR signal around –55 to –60 ppm with line widths of ca. 20–25 ppm, accompanied by several broad signals around 0 ppm (+30 to –30 ppm). The samples showed no marked difference in the chemical shifts of their Si–Si-bonded polymers between solution and solid-state ²⁹Si NMR spectra.

Other possible constructs include a mixture of Si–Si-bonded chain-like and network-like structures (hyperbranched dendritic structures) or a Si–Si-bonded chain-like structure branched with Si-based side chains. However, for 1S, 2R, 2S, and 3, the ²⁹Si resonance between –20 and –32 ppm, which is characteristic of dialkylpolysilanes,^{10b} is not observed (Figure 1). Production of chain-like structures can be ruled out in the Si–Si-bonded structures. Alternatively, the Si–Si-bonded networks may be ladder-like structures comprising fused four-member Si–Si-bonded rings; this type of structure can arise due to the bulkiness of the side groups.¹⁴ However, because ²⁹Si resonances characteristic of the ladder-type oligomers around –35 ppm are not observed,^{14a} the fused four-member rings cannot be dominant and therefore were ruled out.

Solid-state CP/MAS ²⁹Si NMR measurement may allow straightforward characterization of 1S, 2R, 2S, and 3, but the ²⁹Si NMR spectra in solution cannot provide detailed structural information due to the broadness inherent to Si–Si-bonded network polymers with very limited segmental motion. An SNP with *n*-butyl groups (prepared via a similar protocol using Na) showed a broad Raman band around 480 cm^{–1}, typical for amorphous-like Si–Si structures;¹⁵ however, we did not obtain Raman spectra of 1S, 2R, and 2S in order to avoid air oxidation and sample damage during the measurement. Therefore, a

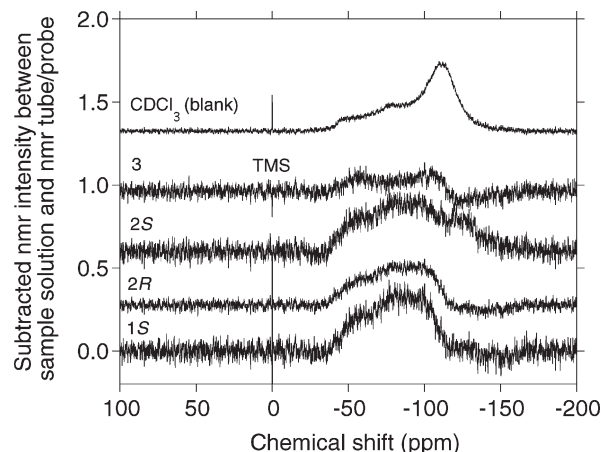


Figure 1. Subtracted ²⁹Si NMR spectra of 1S, 2R, 2S, and 3 with ²⁹Si NMR spectrum of a blank (no polymer) in CDCl₃ at room temperature. The two broad ²⁹Si resonances observed in the blank at –100, –80, and –50 ppm were attributed to ²⁹Si-containing glass in the NMR tube and the probe. Numerical subtraction (KaleidaGraph, Synergy, ver4) of the blank from the samples was carried out to reduce the ²⁹Si NMR signal at –100 ppm.

plausible structure formed from sodium-based reduction of the alkyltrichlorosilanes is an amorphous-like structure,^{10b} in which each Si atom is bonded to three Si atoms and one organic side group. The question remains of whether this polymer skeleton is chirally distorted due to the presence of sterically crowded chiral alkyl side groups. Further chiroptical CD/CPL studies, combined with unpolarized UV–vis and photoluminescence studies, will be needed to answer to this question.

Figure 2 compares the UV–vis spectra, their logarithm spectra, and the PL and PL excitation (PLE) spectra of 1S, 2R, 2S, and 3. It is evident from Figure 2a that 1S, 2R, 2S, and 3 show no clear absorption peaks in the UV–vis region. This is a feature of several previously reported SNPs.¹⁰ However, from the UV–vis spectra shown in Figure 2b (logarithm plots of Figure 2a) the absorption edges of 1S and 3 are shifted to longer wavelengths (ca. 450–500 nm) compared to those of 2R and 2S (ca. 350 nm). In addition, the absorption edge of 1S (ca. 500 nm) is considerably longer than that of 3 (ca. 450 nm). As shown in Figure 2c, 1S, 2R, 2S, and 3 all weakly emit blue-green light consisting of several vibronic PL peaks at room temperature in solution. These PL spectral features are very similar to those of several known SNPs carrying straight and branched side chains, and there are no marked differences in PL spectra between the present four SNPs and previously reported SNPs.^{10,15}

Figure 2d compares the PLE spectra of 1S, 2R, 2S, and 3 in solution. PLE spectra provide selective information on the absorption bands contributing to PL bands that is not provided by the UV–vis absorption spectra. It is evident from Figure 2d that, although the PLE spectrum of 1S has a clear shoulder band near 400 nm, 2R, 2S, and 3 have similar PLE spectra in solution.

Thus, these unpolarized UV–vis, PL, and PLE spectroscopic data merely provide information showing that 1S, 2R, 2S, and 3 adopt very similar local structures, since these UV–vis, PL, and PLE spectra are almost identical to previously reported spectra.¹⁰ However, circularly polarized spectroscopic data, including CD and CPL between 1S, 2R, 2S, and 3 were very different, as follows.

Figure 3a compares the CD and UV–vis spectra of 1S and 3. Three Cotton CD bands are observed for 1S: a positive signal around 250–300 nm ($g_{CD} = +3 \times 10^{-4}$ at 270 nm), a negative signal at 330 nm ($g_{CD} = -1.2 \times 10^{-4}$), and a positive, broad, weak signal around 480 nm ($g_{CD} = +4.8 \times 10^{-3}$). In contrast, no Cotton CD effects were detected in 3. Although the origins of the

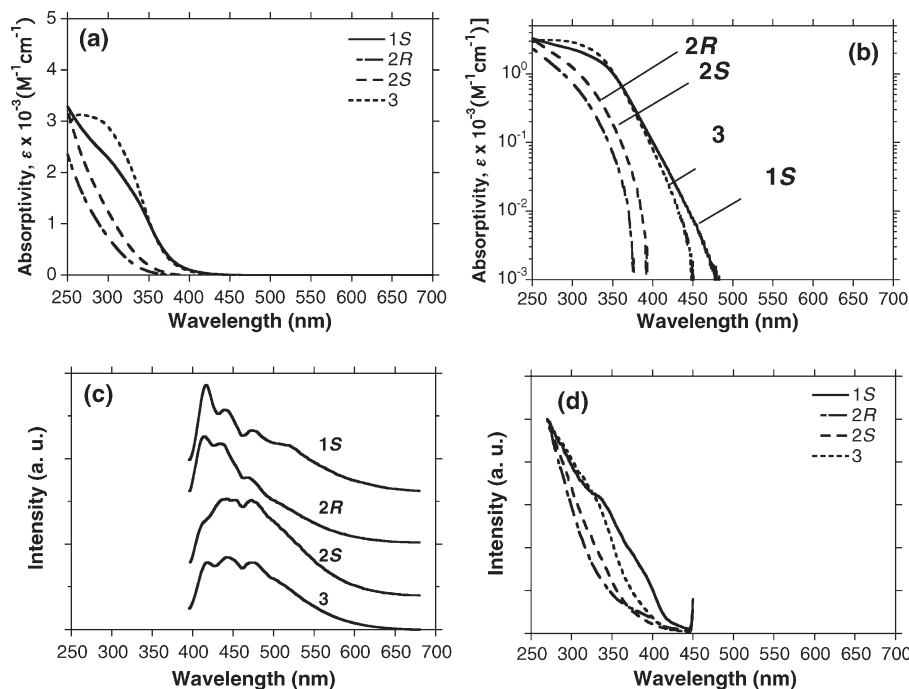


Figure 2. (a) UV-vis spectra, (b) logarithm of UV-vis spectra, (c) PL spectra excited at 360 nm, and (d) PLE spectra of **1S**, **2R**, **2S**, and **3** in THF monitored at 510 nm (UV-vis: $\sim 2.0 \times 10^{-4}$ M per Si repeat unit; PL and PLE: $\sim 1.5 \times 10^{-4}$ M per Si repeat unit).

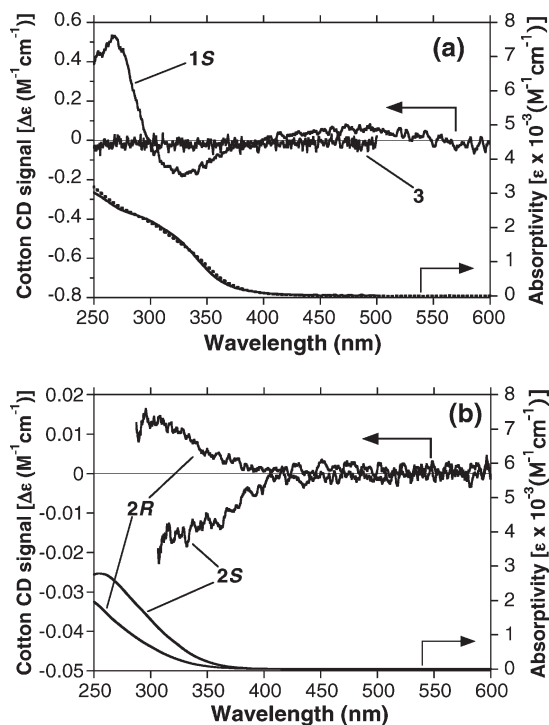


Figure 3. CD (upper lines) and UV-vis (lower lines) spectra of (a) **1S** and **3** and (b) **2R** and **2S** in THF ($\sim 2.0 \times 10^{-4}$ M per Si repeat unit), which were simultaneously obtained with a JASCO J-820 spectropolarimeter.

480, 330, and 270 nm Cotton CD bands are unclear, the 480 and 330 nm CD bands are assumed to arise from two Si σ -Si σ^* transitions with opposite chiralities, as discussed later.¹⁶ The origin of the 270 nm CD band is unclear and will require further studies.

However, it is unclear whether the achiral *n*-pentyl group actually induces a chiral distortion in the Si-Si-bonded network with mirror-image forms, leading to CD-silent chiral structures.

This is because only the (*S*)-chirality of (*S*)-2-methylbutyltrichlorosilane is available from natural sources. To obtain an enantiomeric pair of optically active SNPs, **2S** and **2R** were designed. Although **2S** and **2R** actually exhibited nearly mirror-image Cotton effects in the range of 300–400 nm, the magnitude of their Cotton effects diminished by 1 order of magnitude compared to that of **1S** (Figure 3).

These CD spectroscopic data led to the idea that chiral side chains may induce a certain chirally distorted Si-Si-bonded structure that is incorporated into the network skeleton. The distance between the skeleton and the chiral branching position greatly affects the degree of the distortion: the β -position in the chiral side group affects the Si skeleton significantly more than the γ -position. This tendency is further evident from the marked difference in CPL spectra between **1S** and **2R** excited at 300 nm (Figure 4a). Although **1S** exhibits a positive CPL band that peaks at 570 nm, no clear CPL band from **2R** was detected (nor was a band detected for **2S** or **3**).

The 570 nm CPL band profile of **1S**, including the peak wavelength, does not fit completely with the corresponding unpolarized PL band in the range of 400–800 nm. The signs of the 570 nm CPL band of **1S** and that of the 480 nm CD band are the same, and the absolute magnitude of the 570 nm CPL band ($g_{\text{CPL}} = +5.0 \times 10^{-3}$) is almost identical to that of the 480 nm CD band ($g_{\text{CD}} = +4.8 \times 10^{-3}$). **1S** has at least two major PL components around 420–450 nm and 480–600 nm (Figure S1 in the Supporting Information), depending on excitation wavelength. From Figure 4a, **1S** appears to have a very weak, negative CPL band around 450 nm.

We obtained the subtracted PL spectra between **1S** and **2R** by adjusting the coefficient, as shown in Figure 4b. The peak wavelength of the subtracted PL becomes 570 nm, fitting with that of **1S** CPL band. The band may be connected to the PL band at 480–600 nm in Figure S1. The subtracted PL band with a negative sign at 430 nm is new, and the spectral shape is similar to the corresponding CPL profile of **1S**.

This additional analysis led to the idea that the apparent CPL spectra of **1S** include the negative CPL band around 450 nm and the positive CPL band around 570 nm. To test this idea, a

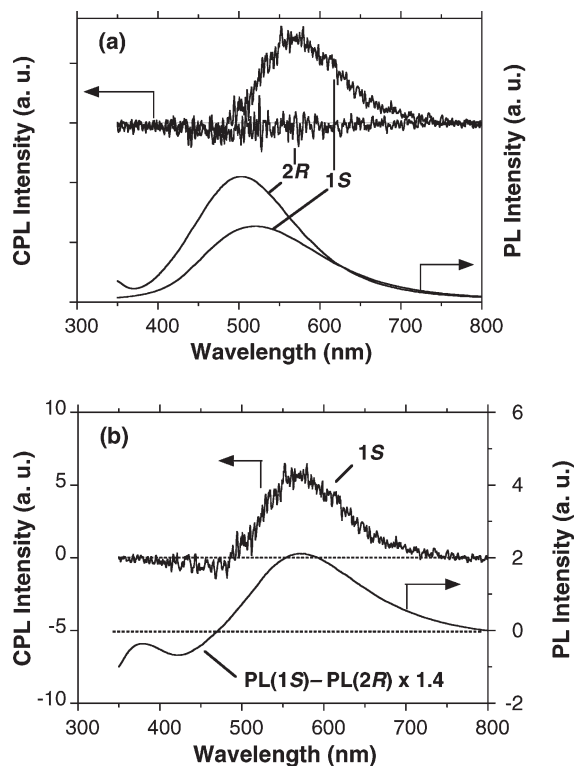


Figure 4. (a) CPL and PL spectra of **1S** and **2R** excited at 300 nm in THF ($\sim 2.0 \times 10^{-3}$ M per Si repeat unit) simultaneously obtained with a JASCO CPL-200 spectrofluoropolarimeter. (b) CPL of **1S** and subtracted PL spectra of **1S** with that of **2R**.

comparison of normalized CPL and CD spectra of **1S** in THF is given in Figure 5a. These data were originally taken from Figures 3a and 4a. As is evident, the intense, positive 570 nm CPL band arises from the positive 480 nm CD band with a Stokes shift of 3300 cm^{-1} , whereas the weak, negative 450 nm CPL band comes from the negative 330 nm CD band with a Stokes shift of 8100 cm^{-1} . From a comparison of the two PLE spectra of **1S** in THF monitored at 560 nm (solid line) and at 520 nm (dotted line) (Figure 5b), a PLE band at 430 nm is evident and may contribute to the 480 nm CD and the 570 nm CPL bands. Very strained fused Si–Si rings with opposite helical chirality incorporated in the **1S** networks are thus assumed to be responsible for the emergence of the negative 330 nm CD, positive 480 nm CD, negative 460 nm CPL, and positive 570 nm CPL bands. The dual chirality with opposite handedness was reported for chain-like Si–Si-bonded polysilane carrying (S)-2-methylbutyl and methyl side groups.¹⁷

These comprehensive spectroscopic analyses led to the conclusion that the CPL band is not due to the whole network skeleton but rather is due to chirally distorted local structures with opposite handedness and different photoexcitation energies; these local structures have been incorporated into the skeleton. Although the chirally distorted structure may be only a small portion of the networks, photoexcited energy above the optical band gaps can relax to the most energetically low photoexcited states. However, the β -branched chiral group actually induces the chirally strained structures responsible for the most energetically low photoexcited states, while in contrast, the γ -branched chiral groups cannot induce the chiral structures responsible for the most energetically low photoexcited states. Therefore, the γ -branched chiral groups cannot contribute the lowest photoexcited states due to the weakness of the side-chain steric effect. The lowest photoexcited states induced by the γ -branched chiral groups may be in achiral structures or in otherwise CD/CPL-silent chiral structures.

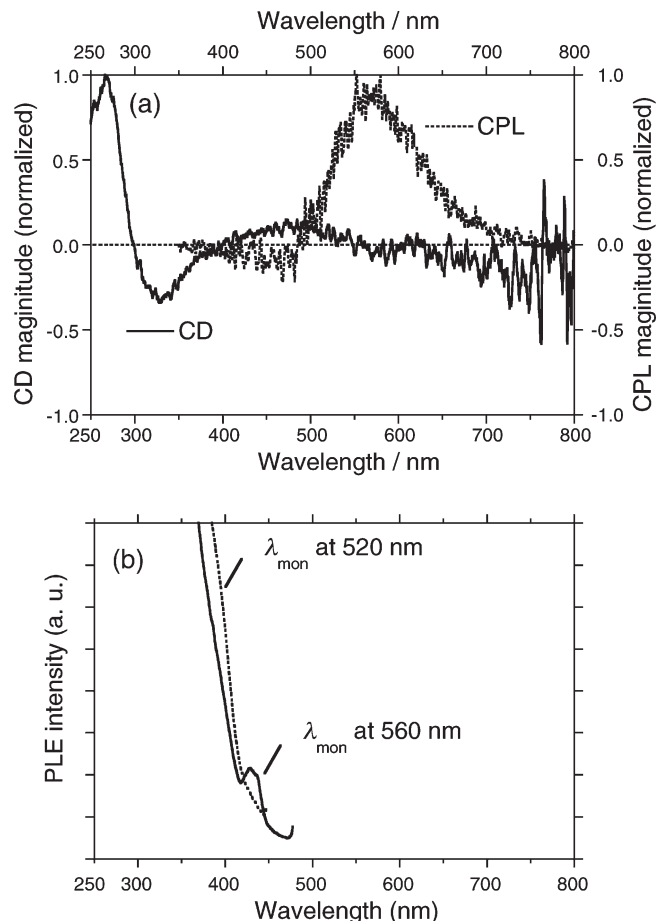


Figure 5. (a) Comparison of normalized CPL (dotted line) and CD (solid line) spectra of **1S** in THF, in which the original data were taken from Figures 3a and 4a. (b) Comparison of PLE spectra monitored at 560 nm (solid line) and 520 nm (dotted line) spectra of **1S** in THF.

Although the Φ value of the PL band in the visible region was $\sim 1\%$ based on the reference 9,10-diphenylanthracene at 25°C ,¹⁸ the CPL property of **1S** might be the first example of CPL among the family of SNPs,¹⁰ including the ladder polysilane.¹⁴ The CPL-functionalized SNP is thus possible to obtain simply via Na-mediated condensation of trichlorosilane bearing β -branched chiral alkyl groups. From our recent finding of various optically inactive SNPs in a controlled vacuum pyrolysis experiment (temperature, time, a trace amount of air),¹⁵ an optically active SNP with β -branched alkyl groups may serve as precursor to Si–Si-bonded ceramics with tunable PL/CPL wavelengths and a higher Φ value.

Conclusions

In summary, we demonstrated the first chiroptical (CPL and CD) spectra for three new SNPs (**1S**, **2R**, and **2S**) bearing chiral alkyl side groups, which were successfully prepared by Na-mediated condensation of the corresponding alkyltrichlorosilanes with the help of crown ether. Although **1S**, **2R**, and **2S** exhibited CD signals in the UV–vis region, only **1S** showed a clear CPL signal in the visible region. A β -branched chiral side chain was needed to provide the intense CPL band in the visible region and to effectively induce chirally distorted Si–Si-bonded structures in SNPs.

Experimental Section

1.1. General. All SNP samples were measured in the liquid state (UV–vis, CD, CPL, PL, and PLE) and were prepared in a

synthetic quartz (SQ)-grade cuvette (path length: 1.0 and 10.0 mm) with a PTFE cap in a glovebox filled with 99.99% pure N_2 gas to avoid any contact with air and moisture. Solutions in spectroscopic grade tetrahydrofuran (Dotite) were used for all measurements.

The CD/UV-vis spectra of the solution state at 25 °C were recorded simultaneously on a JASCO J-820 spectropolarimeter equipped with a Peltier-controlled housing using SQ-grade cuvettes with a path length of 1.0 mm. The scanning conditions were as follows: a scanning rate of 100 nm/min, a bandwidth of 1 nm, a response time of 1 s, and a single accumulation.

UV-vis spectra were also measured independently on a JASCO UV-560 UV-vis-NIR spectrophotometer at 25 °C. The scanning conditions were as follows: a scanning rate of 50 nm/min, a bandwidth of 2 nm, and a response time of 1 s.

PL spectra were measured on a JASCO FP-6500 spectrofluorometer at 25 °C. The scanning conditions were as follows: a scanning rate of 100 nm/min, a bandwidth of 3 nm for excitation, a bandwidth of 3 nm for monitor, and a response time of 2 s. Fluorescence quantum yields were determined relative to 9,10-diphenylanthracene in cyclohexane ($\Phi = 90\%$).¹⁸

CPL spectra were measured on a JASCO CPL-200 spectrofluorometer using SQ-grade cuvettes with a path length of 1.0 mm at room temperature, whereas the instrument was designed to obtain a high S/N ratio by adjusting the angle between the incident and traveling light to 0° with the help of a high-performance notch filter. The scanning conditions were as follows and were averaged from 16 scans: a scanning rate of 100 nm/min, a slit width of 3000 μ m for excitation, a slit width of 3000 μ m for monitor, and a response time of 1 s.

Optical rotation at the Na-d line was measured with JASCO P-1020 and DIP 370 polarimeters using SQ-grade cuvettes with a path length of 1 mm for the neat monomer at room temperature.

NMR spectra were recorded with a JEOL EX-400 spectrometer at 400 MHz for 1H NMR, 100 MHz for ^{13}C , and 80 MHz for ^{29}Si NMR or a Varian Unity 300 spectrometer at 300 MHz for 1H NMR, 75 MHz for ^{13}C , and 60 MHz for ^{29}Si NMR in $CDCl_3$ at ~24 °C. ^{29}Si NMR spectra were recorded using a gated proton decoupled pulse sequence with a relaxation delay of 5 s and were referenced to internal Me_4Si . Chromium(III) acetylacetonate was used as a relaxation reagent for monomers but was not used for SNP samples.

IR spectra were measured on a HORIBA FT-730 spectrometer in transmission mode. Films on a KBr disk (cast in a glovebox) were used. Spectra were recorded with an optical spectral resolution of 4 cm^{-1} , and the results of 16 scans were averaged.

The weight-average molecular weight (M_w) and number-average molecular weight (M_n) were evaluated using gel permeation chromatography (GPC) on Shimadzu A10 instruments, with a PLgel (Varian) 10 μ m mixed-B as the column and HPLC-grade tetrahydrofuran as the eluent at 40 °C, based on a calibration with a polystyrene standard kit (Varian).

The enantiopurities of starting materials and intermediates were determined at the Toray Research Center (Shiga, Japan) using chiral gas chromatography (Spelco, β -DEX-325 and β -DEX-225, 30 m \times 0.25 mm i.d., column oven temperature 70–95 °C, He carrier with 1.2 mL/min).

1.2. Monomer Materials. (*S*)-2-Methylbutyltrichlorosilane (**4**). This was prepared by the literature procedure.¹⁹ To a mixture of 150 mL of dry tetrahydrofuran (Kanto Chemical) and 13.0 g (0.53 mol) of Mg turnings activated with a small amount of 1,2-dibromoethane, 52.9 g (0.496 mol) of (*S*)-2-methylbutyl chloride (TCI, 99.8% *ee*) was added dropwise, and the resulting solution was heated at ~45 °C and stirred. The reaction was allowed to proceed for several hours. To a mixture of 100 g (0.588 mol) of tetrachlorosilane (Shin-Etshu) and 150 mL of dry diethyl ether (Dotite), the freshly prepared Grignard reagent was added dropwise at ~40 °C from a

dropping funnel, and the mixture was allowed to react overnight. After adding about 1 L of *n*-hexane to the reaction mixture, a yellow clear solution containing monomer was collected by reduced filtration. After removal of the solvent and unreacted tetrachlorosilane under reduced pressure (200 Torr), the resulting mixture was carefully distilled. The yield was 47 g (60%): $[\alpha]_D^{24}$ 13.37° (neat) $[\alpha]_D^{20}$ 11.07° (neat)¹⁹; bp 70–75 °C/20 Torr (bp 166–167 °C/755 Torr).¹⁹ ^{29}Si NMR 12.64 ppm. $^{13}C\{^1H\}$ NMR 31.90 (double intensity), 30.38, 21.39, 11.09 ppm. ^{13}C NMR and ^{29}Si NMR spectra are given in Figure S3 of the Supporting Information.

(*S*)-(+)-3,7-Dimethyloctyltrichlorosilane (**5**). This was prepared in line with the literature procedure.²⁰ To a mixture of 100 mL of dry tetrahydrofuran (Kanto Chemical) and 4.2 g (0.18 mol) of Mg turnings activated with a small amount of 1,2-dibromoethane, 33 g (0.15 mol) of (*S*)-(+)-3,7-dimethyloctyl bromide ($[\alpha]_D^{24} = +6.05^\circ$ (neat), 95.0% *ee*) was added dropwise, and the resulting mixture was heated at ~45 °C and stirred. The bromide was prepared at Chemical Soft (Kyoto, Japan) by bromination of (*S*)-(-)-3,7-dimethyloctanol ($[\alpha]_D^{24} = -4.22^\circ$ (neat), 95.9% *ee*), which was prepared by hydrogenation of (*S*)-(-)- β -citronellol (Fluka, $[\alpha]_D^{24} = -4.55^\circ$ (neat), 97.4% *ee*). To a mixture of 50 g (0.294 mol) of tetrachlorosilane (Shin-Etshu) and 150 mL of dry diethyl ether (Kanto Chemical), the freshly prepared Grignard reagent was added dropwise from a dropping funnel at 40 °C, and the reaction was allowed to proceed overnight. After adding about 0.5 L of *n*-hexane to the reaction mixture, a clear yellow solution containing the monomer was collected by reduced filtration. After removal of the solvent and unreacted tetrachlorosilane under reduced pressure (200 Torr), the resulting mixture was distilled. The yield was 23 g (56%): $[\alpha]_D^{24} = +2.25^\circ$ (neat), bp 68–70 °C/0.95 Torr, ^{29}Si NMR 12.65 ppm; $^{13}C\{^1H\}$ NMR 39.22, 36.37, 34.37, 28.91, 27.95, 24.66, 22.69, 22.60, 21.64, 18.99 ppm. ^{13}C NMR and ^{29}Si NMR spectra are given in Figure S4 of the Supporting Information.

(*R*)-(-)-3,7-Dimethyloctyltrichlorosilane (**6**). This was prepared in line with the literature procedure.²⁰ To a mixture of 150 mL of dry diethyl ether (Kanto Chemical) and 6.6 g (0.22 mol) of Mg turnings activated with a small amount of 1,2-dibromoethane, 50.5 g (0.23 mol) of (*R*)-(-)-3,7-dimethyloctyl bromide ($[\alpha]_D^{24} = -5.96^\circ$ (neat), 96.6% *ee*) was added dropwise, and the resulting mixture was refluxed at ~45 °C and stirred. The bromide was prepared at Chemical Soft (Kyoto, Japan) by bromination of (*R*)-(+)-3,7-dimethyloctanol ($[\alpha]_D^{24} = +3.90^\circ$ (neat), 95.7% *ee*), which was prepared by hydrogenation of (*R*)-(+)- β -citronellol (Fluka, $[\alpha]_D^{24} = +4.46^\circ$ (neat), 97.4% *ee*). To a mixture of 14.5 g (0.085 mol) of tetrachlorosilane (Shin-Etshu), 100 mL of dry diethyl ether (Kanto Chemical), and 25 mL of tetrahydrofuran (Kanto Chemical), the fresh Grignard reagent was added dropwise from a dropping funnel at 40 °C and allowed to react overnight. After adding about 1 L of *n*-hexane to the reaction mixture, a clear yellow solution containing monomer was collected by reduced filtration. After removal of the solvent and unreacted tetrachlorosilane under reduced pressure (200 Torr), the resulting mixture was distilled. The yield of the first fraction was 8 g (14%); bp 77–78 °C/1.2 Torr; $[\alpha]_D^{24} = -2.54^\circ$ (neat). ^{29}Si NMR 12.65 ppm. ^{29}Si NMR spectrum is given in Figure S5 of the Supporting Information.

n-Pentyltrichlorosilane (**7**). This was purchased from Shin-Etsu and distilled prior to use bp 60–61 °C/15 Torr. The ^{29}Si NMR spectrum is given in Figure S6 of the Supporting Information.

1.3. Polymeric Materials. *Syntheses of Representative Example, Poly[(S)-2-methylbutylsilylene] (IS).* In a nitrogen atmosphere, 0.45 g (19.4 mmol) of sodium was dispersed in a mixture of 10 mL of boiling toluene and 17.1 mg (0.0972 mmol) of 12-crown-4 (Aldrich) by vigorous mechanical stirring. Subsequently, 1.00 g (4.86 mmol) of **4** was added dropwise (*caution: a strongly*

exothermic reaction occurs). The reaction mixture was refluxed for 1 h during which a purple color developed. After cooling to room temperature, the glass vessel was transferred to a glovebox filled with 99.99% pure nitrogen gas. The reactant mixture was then filtered using a PTFE membrane filter (0.45 μm pore size) to remove sodium chloride and unreacted sodium. The filtrate was further purified by precipitation with dry acetone several times. The isolated yield, color, state, and GPC information for **1S**, **2R**, **3S**, and **3** are given in Table 1.

1.4. ^1H NMR and ^{29}Si NMR Charts and IR Spectra of **1S, **2R**, **2S**, and **3**.** ^1H NMR, ^{13}C NMR, and ^{29}Si NMR spectra and IR spectra of **1S**, **2R**, **2S**, and **3** are displayed in Figures S7–S10 of the Supporting Information.

1.5. Optical Spectra of **1S, **2R**, **2S**, and **3** in THF at 25 °C.** Detailed PL spectra of **1S**, **2R**, **2S**, and **3** with different excitation wavelengths are displayed in Figure S1 of the Supporting Information. Detailed PLE spectra of **1S**, **2R**, **2S**, and **3** with different monitor wavelengths are displayed in Figure S2 of the Supporting Information.

Acknowledgment. This work was supported by a Grant-in-Aid for Science Research in a Priority Area “Super-Hierarchical Structures (17067012)” from MEXT, Japan (FY2005–2008), and was supported by the Nippon Sheet Glass Foundation for Materials Science and Engineering (FY2009). The authors thank Drs. Hisao Yanagi, Atsushi Ikeda, Yasuchika Hasegawa, Masanobu Naito, Kotohiro Nomura, and Hisanari Onouchi for their stimulating discussions and fruitful comments. Yoko Nakano is gratefully acknowledged for her technical guidance in CPL and CD measurements. M.F. thanks Dr. Wei Zhang at Soochow (Suzhou) University (a visiting researcher at NAIST, FY2009–2010) for fruitful discussions and for critical reading of the entire text in its original form.

Supporting Information Available: NMR, IR, and additional PL and PLE spectra of materials studied in this work. This material is available free of charge via the Internet at <http://pubs.acs.org>.

References and Notes

- (1) (a) Green, M. M.; Peterson, N. C.; Sato, T.; Teramoto, A.; Cook, R.; Lifson, S. *Science* **1995**, *268*, 1860–1866. (b) Peeters, E.; Christiaens, M. P. T.; Janssen, R. A.; Schoo, H. F. M.; Dekkers, H. P. J. M.; Meijer, E. W. *J. Am. Chem. Soc.* **1997**, *119*, 9909–9910. (c) Chen, S. H.; Katsis, D.; Schmid, A. W.; Mastrangelo, J. C.; Tsutsui, T.; Blanton, T. N. *Nature* **1999**, *397*, 506–508. (d) Chen, H. P.; Katsis, D.; Mastrangelo, J. C.; Chen, S. H.; Jacobs, S. D.; Hood, P. J. *Adv. Mater.* **2000**, *12*, 1283–1286. (e) Nakashima, H.; Koe, J. R.; Torimitsu, K.; Fujiki, M. *J. Am. Chem. Soc.* **2001**, *123*, 4847–4848. (f) Nakako, H.; Nomura, R.; Masuda, T. *Macromolecules* **2001**, *34*, 1496–1502. (g) Schenning, A. P. H. J.; Jonkheijm, P.; Peeters, E.; Meijer, E. W. *J. Am. Chem. Soc.* **2001**, *123*, 409–416. (h) Fujiki, M. *J. Am. Chem. Soc.* **2000**, *122*, 3336–3343. (i) Saxena, A.; Guo, G.; Fujiki, M.; Yang, Y.; Ohira, A.; Okoshi, K.; Naito, M. *Macromolecules* **2004**, *37*, 3081–3083. (j) Tang, H.-Z.; Novak, B. M.; He, J.; Polavarapu, P. L. *Angew. Chem., Int. Ed.* **2005**, *44*, 7298–7301. (k) Satrijo, A.; Meskers, S. C. J.; Swager, T. M. *J. Am. Chem. Soc.* **2006**, *128*, 9030–9031. (l) Lakhwani, G.; Meskers, S. C. J.; Janssen, R. A. J. *J. Phys. Chem. B* **2007**, *111*, 5124–5131. (m) Luijten, J.; Vorenkamp, E. J.; Schouten, A. J. *Langmuir* **2007**, *23*, 10772–10778. (n) Cipparrone, G.; Pagliusi, P.; Provenzano, C.; Shibaev, V. P. *Macromolecules* **2008**, *41*, 5992–5996. (o) Yashima, E.; Maeda, K.; Furusho, Y. *Acc. Chem. Res.* **2008**, *41*, 1166–1180.
- (2) (a) van Delden, R. A.; Huck, N. P. M.; Piet, J. J.; Warman, J. M.; Meskers, S. C. J.; Dekkers, H. P. J. M.; Feringa, B. L. *J. Am. Chem. Soc.* **2003**, *125*, 15659–15665. (b) Spano, F. C.; Meskers, S. C. J.; Hennebicq, E.; Beljonne, D. *J. Am. Chem. Soc.* **2007**, *129*, 7044–7054. (c) Petoud, S.; Muller, G.; Moore, E. G.; Xu, J.; Sokolnicki, J.; Riehl, J. P.; Le, U. N.; Cohen, S. M.; Raymond, K. N. *J. Am. Chem. Soc.* **2007**, *129*, 77–83. (d) Do, K.; Muller, F. C.; Muller, G. *J. Phys. Chem.* **2008**, *112*, 6789–6793. (e) Lunkley, J. L.; Shirotani, D.; Yamanari, K.; Kaizaki, S.; Muller, G. *J. Am. Chem. Soc.* **2008**, *130*, 13814–13815.
- (3) (a) Yao, H.; Miki, K.; Nishida, N.; Sasaki, A.; Kimura, K. *J. Am. Chem. Soc.* **2005**, *127*, 15536–15543. (b) Imai, Y.; Kawano, K.; Nakano, Y.; Kawaguchi, K.; Harada, T.; Sato, T.; Fujiki, M.; Kuroda, R.; Matsubara, Y. *New J. Chem.* **2008**, *32*, 1110–1112. (c) Imai, Y.; Murata, K.; Asano, N.; Nakano, Y.; Kawaguchi, K.; Harada, T.; Sato, T.; Fujiki, M.; Kuroda, R.; Matsubara, Y. *Cryst. Growth Des.* **2008**, *8*, 3376–3379. (d) Elliott, S. D.; Moloney, M. P.; Gun'ko, Y. K. *Nano Lett.* **2008**, *8*, 2452–2457.
- (4) Berova, N.; Nakanishi, K.; Woody, R. W. *Circular Dichroism – Principles and Applications*, 2nd ed.; Wiley-VCH: New York, 2000.
- (5) For reviews: (a) Brus, L. *J. Phys. Chem.* **1994**, *98*, 3575–3581. (b) Takeda, K.; Shiraishi, K. *Comments Condens. Matter Phys.* **1997**, *18*, 91–133. (c) Matsumoto, N. *Jpn. J. Appl. Phys.* **1998**, *37*, 5425–5436. (d) Watanabe, A. *J. Organomet. Chem.* **2003**, *685*, 122–133.
- (6) (a) Furukawa, S.; Miyasato, T. *Phys. Rev. B* **1988**, *38*, 5726–5729. (b) Takagi, H.; Ogawa, H.; Yamazaki, Y.; Ishizaki, A.; Nakagiri, T. *Appl. Phys. Lett.* **1990**, *56*, 2379–2381. (c) Kanemitsu, Y.; Ogawa, T.; Shiraishi, K.; Takeda, K. *Phys. Rev. B* **1993**, *48*, 4883–4886.
- (7) (a) Lehmann, V.; Gösele, U. *Appl. Phys. Lett.* **1991**, *58*, 856–858. (b) Cullis, A.; Canham, L. T. *Nature Phys.* **1991**, *353*, 335–338.
- (8) (a) Grom, G. F.; Lockwood, D. J.; McCaffrey, J. P.; Labbe, H. J.; Fauchet, P. M.; White, B., Jr.; Diener, J.; Kovalev, D.; Koch, F.; Tsybeskov, L. *Nature* **2000**, *407*, 358–361. (b) Gelloz, B.; Kojima, A.; Koshida, N. *Appl. Phys. Lett.* **2005**, *87*, 031107. (c) English, D. S.; Pell, L. E.; Yu, Z.; Barbara, P. F.; Korgel, B. A. *Nano Lett.* **2002**, *2*, 681–685. (d) Li, X.; He, Y.; Swihart, M. T. *Langmuir* **2004**, *20*, 4720–4727. (e) Liu, S.-M.; Yang, Y.; Sato, S.; Kimura, K. *Chem. Mater.* **2006**, *18*, 637–642. (f) Choi, J.; Wang, N. S.; Reipa, V. *Langmuir* **2007**, *23*, 3388–3394. (g) Zhang, X.; Brynda, M.; Britt, R. D.; Carroll, E. C.; Larsen, D. S.; Louie, A. Y.; Kaulzarich, S. M. *J. Am. Chem. Soc.* **2007**, *129*, 10668–10669. (h) Hua, F.; Swihart, M. T.; Ruckenstein, E. *Langmuir* **2006**, *22*, 6054–6062. (i) Hanaizumi, O.; Ono, K.; Ogawa, Y. *Appl. Phys. Lett.* **2003**, *82*, 538–540. (j) Nayfeh, M.; Mitás, L. In *Nano-silicon*; Kumar, V., Ed.; Elsevier: Oxford, 2008; Chapter 1.
- (9) (a) Miller, R. D.; Michl, J. *Chem. Rev.* **1989**, *89*, 1359–1410. (b) West, R. In *The Chemistry of Organic Silicon Compounds*; Patai, S.; Rappoport, Z., Eds.; John Wiley and Sons: New York, 1989. (c) Fujiki, M. *Macromol. Rapid Commun.* **2001**, *22*, 539–563. (d) Fujiki, M.; Koe, J. R.; Terao, K.; Sato, T.; Teramoto, A.; Watanabe, J. *Polym. J.* **2003**, *35*, 297–344. (e) Dellaportas, P.; Holder, S. J.; Jones, R. G. *Macromol. Rapid Commun.* **2002**, *23*, 99–103. (f) Dellaportas, P.; Holder, S. J.; Jones, R. G. *J. Am. Chem. Soc.* **2006**, *128*, 12418–12419.
- (10) (a) Bianconi, P. A.; Weidman, T. W. *J. Am. Chem. Soc.* **1988**, *110*, 2342–2344. (b) Bianconi, P. A.; Schilling, F. C.; Weidman, T. W. *Macromolecules* **1989**, *22*, 1697–1704. (c) Wilson, W. L.; Weidman, T. W. *J. Phys. Chem.* **1991**, *95*, 4568–4572. (d) Smith, D. A.; Freed, C. A.; Bianconi, P. A. *Chem. Mater.* **1993**, *5*, 245–247. (e) Cleij, T. J.; Tsang, S. K. Y.; Jenneskens, L. W. *Macromolecules* **1999**, *32*, 3286–3294. (f) Furukawa, K.; Fujino, M.; Matsumoto, N. *Macromolecules* **1990**, *23*, 3423–3426.
- (11) Brandt, M. S.; Vogg, G.; Stutzmann, M. In *Silicon Chemistry*; Jutzi, P.; Schubert, U., Eds.; Wiley-VCH: Weinheim, 2003; Chapter 15.
- (12) Lu, Z. H.; Lockwood, D. J.; Baribeau, J.-M. *Nature* **1995**, *378*, 258–260.
- (13) (a) Watanabe, A.; Miike, H.; Tsutsumi, Y.; Matsuda, M. *Macromolecules* **1993**, *26*, 2111–1116. (b) Maxka, J.; Cgrusciel, J.; Sasaki, M.; Matyjaszewski, K. *Macromol. Symp.* **1994**, *77*, 79–92. (c) Watanabe, A.; Tsutsumi, Y.; Matsuda, M. *Synth. Met.* **1995**, *74*, 191–196. (d) Sasaki, M.; Matyjaszewski, K. *J. Polym. Sci., Part A: Polym. Chem.* **1995**, *33*, 771–778. (e) van Walree, C. A.; Cleij, T. J.; Jenneskens, L. W.; Vlietstra, E. J.; van der Laan, G. P.; de Haas, M. P.; Lutz, E. T. G. *Macromolecules* **1996**, *29*, 7362–7373. (f) Toyoda, S.; Fujiki, M. *Macromolecules* **2001**, *34*, 2630–2634.
- (14) (a) Matsumoto, H.; Miyamoto, H.; Kojima, N.; Nagai, Y. *J. Chem. Soc., Chem. Commun.* **1987**, 1316–1317. (b) Kyushin, S.; Ueta, Y.; Tanaka, R.; Matsumoto, H. *Chem. Lett.* **2006**, *35*, 182–183. (c) Kyushin, S.; Matsumoto, H. *Adv. Organomet. Chem.* **2003**, *49*, 133–166.
- (15) Fujiki, M.; Kawamoto, Y.; Kato, M.; Fujimoto, Y.; Saito, T.; Hososhima, S.; Kwak, G. *Chem. Mater.* **2009**, *21*, 2459–2466.
- (16) Snatzke, G. In *Chirality – From Weak Bosons to the α -Helix*; Janoscheck, R., Ed.; Springer: Berlin, 1991; Chapter 4.
- (17) Fujiki, M. *J. Am. Chem. Soc.* **1994**, *116*, 11976–11981.
- (18) Eaton, D. F. *Pure Appl. Chem.* **1988**, *60*, 1107–1114.
- (19) Spialter, L.; O'Brien, D. H. *J. Org. Chem.* **1966**, *31*, 3048–3049.
- (20) Fujiki, M.; Koe, J. R.; Motonaga, M.; Nakashima, H.; Terao, K.; Teramoto, A. *J. Am. Chem. Soc.* **2001**, *123*, 6253–6261.